

# Densification and Microstructure Development of Alumina/Y-TZP Composite Powder (Y-TZP-rich) Compacts

J. L. Shi & T. S. Yen

State Key Laboratory of High Performance Ceramics and Superfine Microstructure, Shanghai Institute of Ceramics, 1295 Ding-Xi Road, Shanghai 200050, People's Republic of China

(Received 25 November 1993; revised version received 1 June 1994; accepted 11 August 1994)

## Abstract

*Al<sub>2</sub>O<sub>3</sub>/Y-TZP composite powders (Y-TZP-rich) were prepared by ball milling submicron-sized alumina and coprecipitated nano-sized Y-TZP powders. The densification behavior of the composite powder compacts is studied and it is shown that the shrinkage rate is reduced at lower temperatures and the composites continue to shrink at elevated temperatures compared to single phase tetragonal Y-TZP. Compacts of the composite powders isostatically pressed at 250 MPa at room temperature show duplex pore size distributions due to the presence of alumina, and it is these unusual pore size distributions, rather than the stresses arising from the differential sintering of the secondary particles that are believed to be the source of the retarded densification during constant rate heating. In spite of the retarded densification behavior, the composite powder compacts containing not higher than 30 vol.% alumina, can be sintered in 2 h to above 98% of the theoretical density at 1550°C.*

## 1 Introduction

Alumina/Y-TZP particulate composites are of great interest because of their improved mechanical properties, such as strength, toughness and hardness.<sup>1–5</sup> In particular, alumina-doped Y-TZP materials show unusually high fracture strength.<sup>5</sup> These composites, however, show limited densification when pressureless sintered<sup>4–6</sup> and require hot-pressing or post-hipping to achieve density levels suitable for practical application.

Conventionally, the phase of higher content and smaller particle size is termed the matrix phase and the one of lower content and larger particle size is the secondary phase. The sintering behavior of particulate composites has been studied extensively, and it is well known that the densification

of matrices (or composites) is retarded by secondary large particles (inclusions).<sup>6–13</sup> Numerous models have been proposed to account for this retarded densification of the matrix by the secondary phase.<sup>14–21</sup> The early models<sup>14–17</sup> proposed a hydrostatic tensile stress (back stress), believed to counter the normal sintering stress, as the main factor affecting densification. It was later proposed<sup>18,19</sup> that the tensile stress was too small to be the source of retarded densification; instead, the enlargement of pre-existing cracks in the compacts as a result of the tensile stress during sintering was considered to retard densification. Recently a numerical model<sup>20,21</sup> stated that the dense non-deformable region around high-aspect ratio reinforcements and between closely spaced reinforcements constrained the shrinkage of the adjacent, porous matrix, and thus led to the formation of large voids and cracks. These models, in spite of differences in the densification retardation mechanisms, all rely on the effect of stresses due to the presence of the secondary particles.

The retarded densification of particulate composites has also been attributed to the suppressed grain growth of the matrix grains during sintering,<sup>22,23</sup> because it was believed that grain growth enhanced densification.<sup>24</sup>

The proposed stress models are based mostly on the experimental results for composites with very large inclusions as secondary phases, i.e. with size ratios of the inclusions to matrix larger than 100.<sup>10,11,13,21</sup> However, many practical particulate composite systems do not use large size secondary phase particles, so as to avoid large defects in microstructure. For example, in the Al<sub>2</sub>O<sub>3</sub>/Y-TZP system the size ratio of the second phase to matrix is generally less than 10. For systems of inclusion size to matrix size ratios of around 10, the retarded densification may not be caused by stress alone, as the stresses brought about by the

secondary phase are somewhat limited for small secondary particle size and size ratio.

Recent reports<sup>25,26</sup> have shown that the back stress model<sup>17</sup> does not work in the  $\text{ZrO}_2$  inclusions/ $\text{ZnO}$  matrix system. In their system, the size ratios of  $\text{ZrO}_2$  to  $\text{ZnO}$  matrix varied from about 3 to 30. They proposed that in addition to the interaction between secondary particles and the matrix, the packing properties near the secondary particles may contribute to the retarded densification in the matrix.

In the present study on  $\text{Al}_2\text{O}_3/\text{Y-TZP}$  composites, a possible alternative factor affecting densification of composites is identified and a microstructural model based on this finding is introduced.

## 2 Experimental

Alumina powder (Sumitomo Co., AKP-50) with an average particle size of about  $0.23\ \mu\text{m}$  as measured by gravity sedimentation by the supplier was used. Y-TZP (3 mol% yttria stabilized tetragonal zirconia polycrystals) powder was obtained by a coprecipitation method using zirconium oxychloride and yttrium chloride as starting materials and ammonia as the precipitation medium. The coprecipitation process is described briefly as follows:<sup>27</sup> (1) a mixed solution of zirconium oxychloride and yttria chloride with proper  $\text{Y}^{3+}/\text{Zr}^{4+}$  was prepared; (2) the mixed solution was added to an ammonia solution which resulted in coprecipitation: the pH value was kept above 9.5; (3) the coprecipitates were repeatedly washed to remove  $\text{Cl}^-$  until the  $\text{Cl}^-$  content in the filtrate became less than 10 ppm; (4) the coprecipitated cake was dispersed and dried in an oven at  $110^\circ\text{C}$ ; (5) the powder was calcined at  $750^\circ\text{C}$  for 120 min. To avoid the formation of hard agglomerates, the coprecipitates of mixed hydroxide were thoroughly dispersed with a 30 min ultrasonic treatment before drying and calcination. The average primary particle size (equivalent to the crystallite size) of the 3Y-TZP powder is about 22 nm as measured by the X-ray diffraction line broadening method and/or by measuring the specific surface area by BET method (assuming a spherical shape for the particles).<sup>28</sup> Alumina-Y-TZP composite powders were prepared via ball milling for 4 h in a plastic jar using alumina balls as milling media. Five batches of the composite powders were prepared, containing 0, 10, 20, 30, and 40 vol.% alumina, and labelled accordingly as ZA0, ZA10, ZA20, ZA30, and ZA40 respectively. Figure 1 is a typical TEM photomicrograph of ZA30 powder after ball milling, showing a mixture of submicro-sized  $\text{Al}_2\text{O}_3$  and nano-sized Y-TZP crystallites.



Fig. 1. TEM micrograph of mixed  $\text{Al}_2\text{O}_3/\text{Y-TZP}$  composite powder.

The composite powders were uniaxially dry pressed at 50 MPa, followed by cold isostatic pressing at 250 MPa, and the binder (1.5% polyvinyl alcohol) in the green compacts was burnt out by heating up to  $700^\circ\text{C}$  for 2 h. The pore size distributions of the pressed compacts were measured by mercury porosimetry (Model 9200, Micromeritics, USA) which detects pores in the size range  $300\ \mu\text{m}$ –3 nm.

The shrinkage behavior of the samples was measured with a dilatometer at a constant heating rate of  $10^\circ\text{C}/\text{min}$  up to  $1550^\circ\text{C}$ , followed by holding at this temperature for 2 h. Densities of the sintered samples were measured by the Archimedes method in distilled water. The microstructure of the sintered bodies was observed with scanning electron microscopy (SEM, EPMA-8705, Shimadzu) on the ground and polished surfaces after thermal etching at  $1300^\circ\text{C}$  for 150 min.

## 3 Results

### 3.1 Duplex pore size distributions in the compacts

Figure 2 shows the pore size distributions of the composite powder compacts after isostatic pressing at 250 MPa. The pure Y-TZP compact exhibits pore size distribution with only one peak illustrating an agglomerate-free state in the compact.<sup>27</sup> Addition of alumina to the Y-TZP powders results in two peaks in the pore size distribution (a duplex distribution). The peaks at smaller pore sizes (Pore I  $\leq 0.03\ \mu\text{m}$ ) are the inter-primary particle pores of the zirconia particles as the zirconia powders are much finer than the alumina powder. Those at larger size (Pore II  $> 0.03\ \mu\text{m}$ ) are the result of the presence of the alumina particles. There are two possibilities for the larger pores. They may be formed between alumina particles

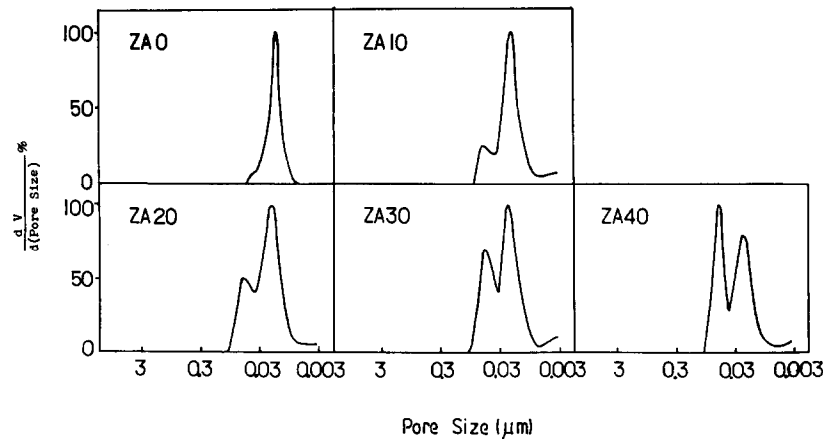


Fig. 2. Pore size distributions of the composite powder compacts at 250 MPa.

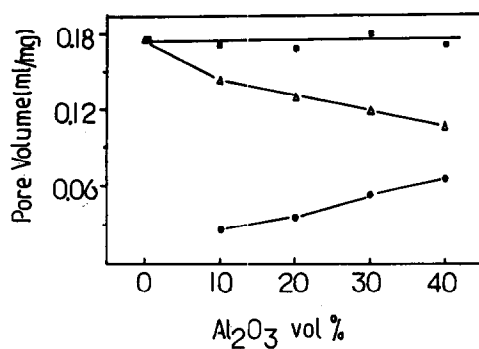


Fig. 3. Volume contents of (■) total pores, (Δ) Pore I and (●) Pore II in the composite powder compacts.

(inter-alumina particle pores) and/or formed between alumina particles and Y-TZP matrix (inter-alumina-zirconia particle pores). The former are predicted to be present since agglomerates may also develop from the submicron-sized  $\text{Al}_2\text{O}_3$  particles if the agglomerates are not fully dispersed especially when the alumina content is high, the latter are sure to exist because the  $\text{Al}_2\text{O}_3$  particles or agglomerates are surrounded by nano-sized Y-TZP particles at relatively low contents.

Increasing alumina content in the composite powders leads to a volume increase of porosity (Pore II) and a decrease of porosity (Pore I), while the total pore volume remains essentially

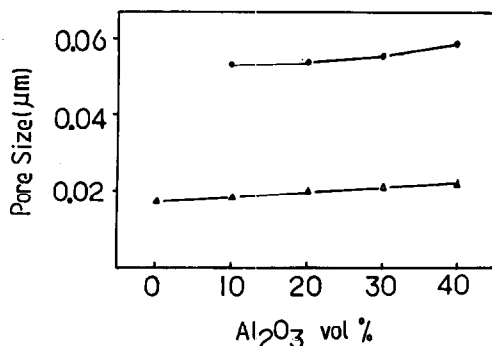


Fig. 4. Effect of alumina content on the size of (Δ) Pore I and (●) Pore II in the compacts.

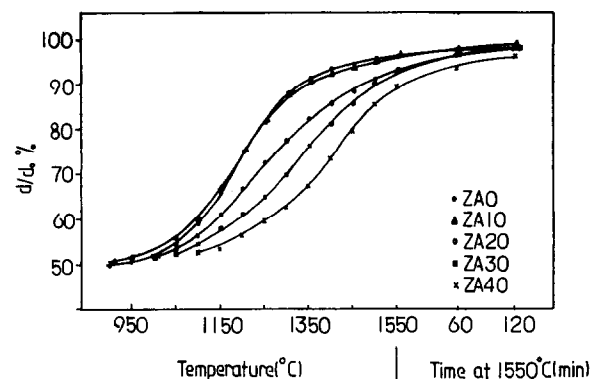


Fig. 5. Densification curves of the composites during constant rate heating of  $10^\circ\text{C}/\text{min}$  up to  $1550^\circ\text{C}$  and holding at  $1550^\circ\text{C}$  for 2 h.

unaffected, as shown in Fig. 3. In addition to the pore volume, the average pore sizes (Pores I and II) also increase slightly along with increasing alumina content, as shown in Fig. 4.

### 3.2 Retarded densification of the composite

The densification curves in Fig. 5 show the retarded densification behavior due to the presence of alumina, especially at and beyond 20 vol.%. At the lower temperatures, the shrinkage rates decrease with the increase of alumina content. At higher temperatures and during the high temperature hold, the shrinkage rates increase with the increase of alumina content, as shown in Fig. 6 and, more clearly, in Fig. 7. Although similar final densities can be obtained for composite compacts containing not more than 30 vol.% of alumina (see Fig. 5) when sintered at  $1550^\circ\text{C}$  for 2 h, the shrinkage rates during constant rate heating and holding depend on the alumina content in the composites.

### 3.3 Pore structure change during densification

During sintering, the pore volume and size change as densification proceeds. At relatively low tem-

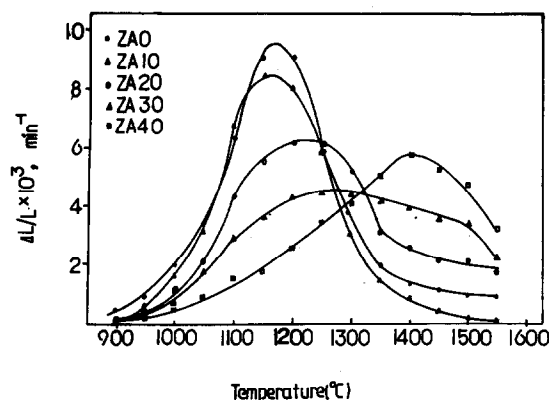


Fig. 6. Shrinkage rate versus temperature during constant rate heating for the composites.

peratures, the change is due mainly to the volume decrease and slight size increase of Pore I. This corresponds to the shrinkage of the green compacts in the early stages of sintering, especially for those with low content of alumina. Beyond 1150°C, there is only one peak (Pore II and size increased Pore I) left as shown in Fig. 8, and the volume diminution (Fig. 9) and size increase (Fig. 10) of the pores continue to relatively high temperatures, which is more evident for the materials with a higher alumina content.

### 3.4 Microstructure development of the composites

Figure 11 shows the photomicrographs of  $\text{Al}_2\text{O}_3/\text{Y-TZP}$  composite bodies sintered at 1550°C for 2 h. For single phase Y-TZP the microstructure is uniform and the grains are submicron-sized (0.3–0.5  $\mu\text{m}$ ). Addition of  $\text{Al}_2\text{O}_3$  particles to the composites leads to a less uniform microstructure: the black particles of relatively large size are  $\text{Al}_2\text{O}_3$  and the matrix is Y-TZP, as verified by energy dispersive spectroscopy. Both  $\text{Al}_2\text{O}_3$  and Y-TZP matrix grains in the sintered bodies have grown compared to the powder forms: Y-TZP grains have grown as in the single phase materials by a factor of greater than 10 and the grain sizes are almost independent of the alumina content. The  $\text{Al}_2\text{O}_3$  grain sizes became larger as the  $\text{Al}_2\text{O}_3$  content increased, and the rate of increase depended on  $\text{Al}_2\text{O}_3$  content. So the size ratio of alumina to Y-TZP particles becomes larger for higher  $\text{Al}_2\text{O}_3$  content in the final sintered bodies. Even for ZA40, however, the size ratios in the final sintered bodies were less than 10, that is to say that  $\text{Al}_2\text{O}_3$  grains grew at a slower rate than Y-TZP.

In spite of the grain size differences for different  $\text{Al}_2\text{O}_3$  contents, the sintered bodies were dense and no pores were formed in the vicinity of the larger  $\text{Al}_2\text{O}_3$  particles, in contrast to results of Tuan<sup>10</sup> and Sudre<sup>13,21</sup> in their particular systems.

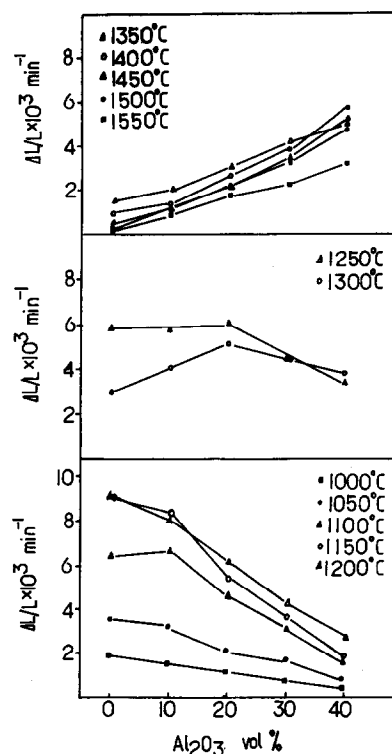


Fig. 7. Shrinkage rate versus alumina content during constant rate heating at various temperatures.

## 4 Discussion

### 4.1 Densification retardation by duplex pore size distribution

The effect of bimodal pore size distributions on the viscous sintering of single phase uniform gel compacts has been discussed by Scherer.<sup>14</sup> Altered sintering stress in this system results from the interaction between large and small pores. However, a gel compact with uniform composition is different from a particulate system of multiphase form

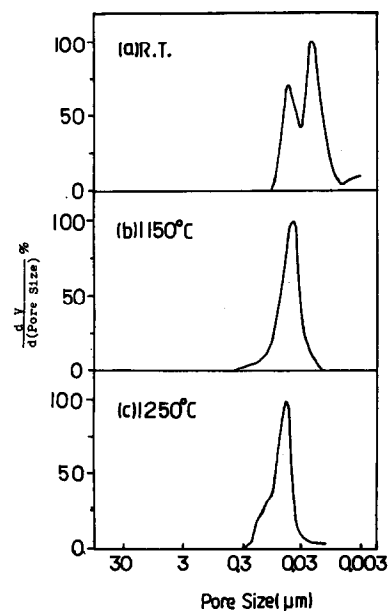


Fig. 8. Pore size distributions of 30 vol.%  $\text{Al}_2\text{O}_3/\text{Y-TZP}$  composites during constant rate heating at (a) room temperature, (b) 1150°C, (c) 1250°C.

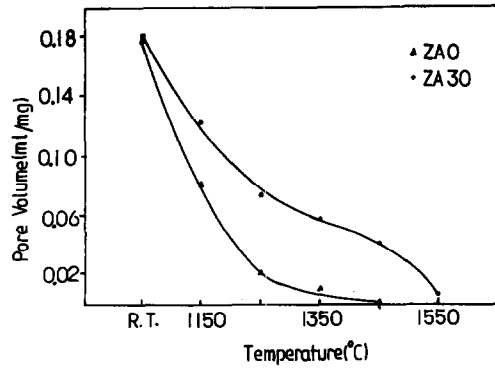


Fig. 9. Pore volume versus temperature during constant rate heating.

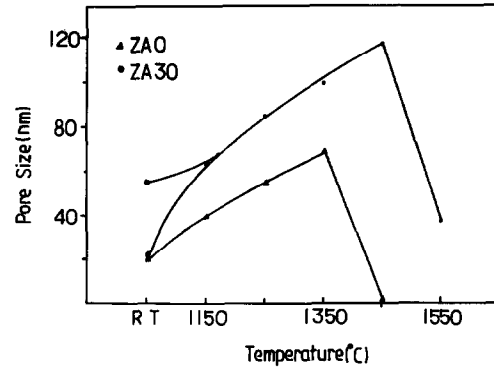


Fig. 10. Pore size versus temperature during constant rate heating.

such as has been studied in this paper. The viscous sintering mechanism of a single phased gel without phase and/or grain boundaries cannot be used to explain the solid state sintering behavior of the present multiphased particulate system.

The presence of large pores in the compacts implies that the particle packing conditions in the multiphase system have been changed. The pores of large sizes (Pore II) may be formed among large alumina particles (inter-alumina particle pores,

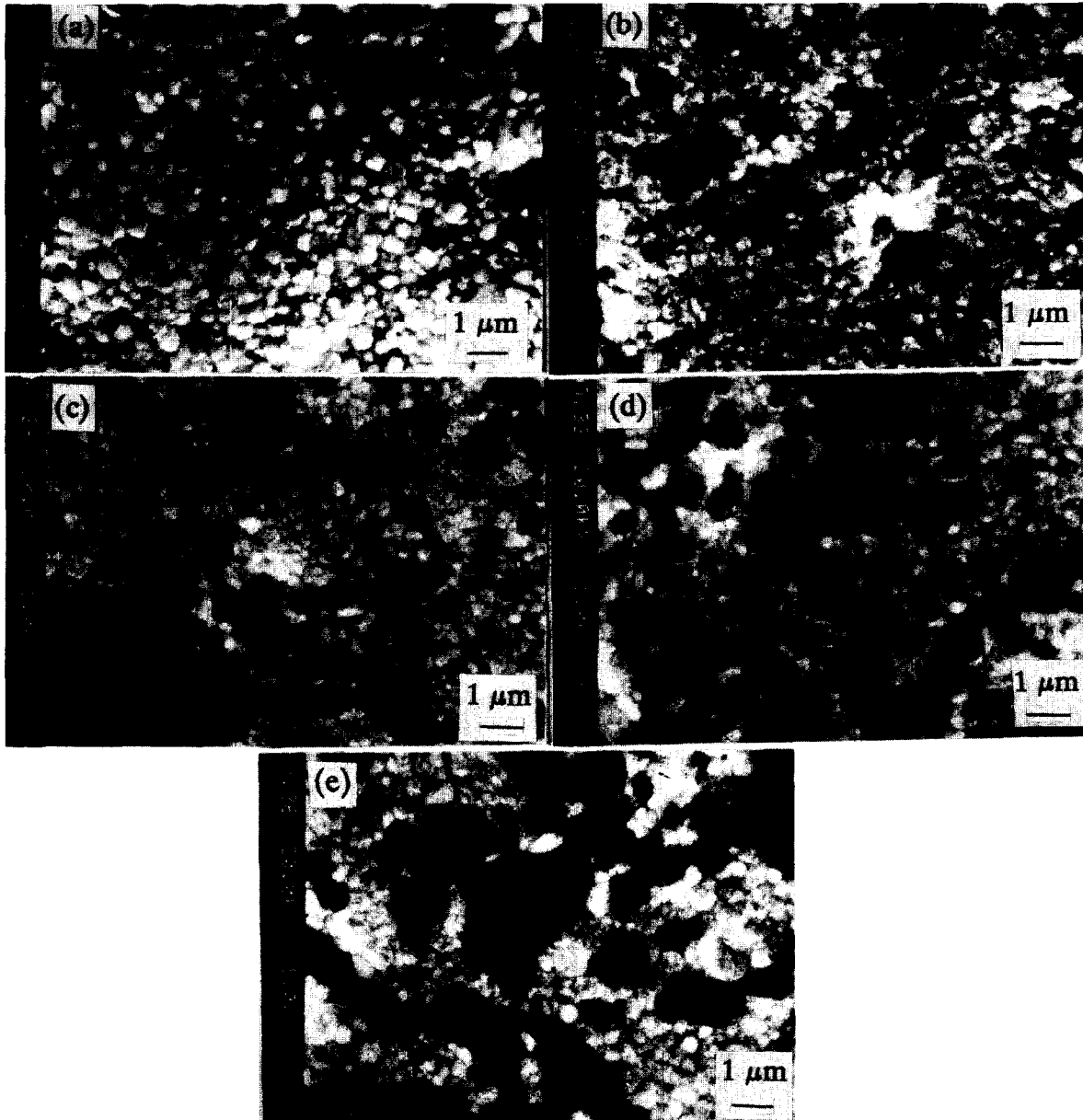


Fig. 11. SEM micrographs on polished and thermally etched surfaces of sintered composite bodies at 1550°C for 120 min, containing (a) 0, (b) 10, (c) 20, (d) 30 and (e) 40 vol.%  $\text{Al}_2\text{O}_3$ .

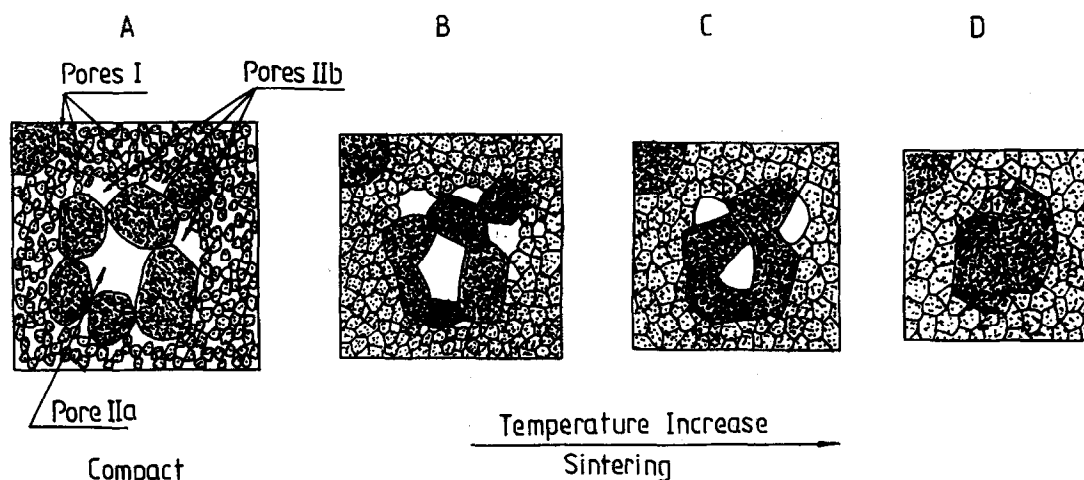


Fig. 12. Microstructure model for the removal of different kinds of pores; (A) pores in compacts; (B) removal of Pore I at relatively low temperature; (C) Pore IIa begin to shrink and Pore IIb become unstable due to the grain growth of Y-TZP as temperature increases, and (D) Pores II were eliminated at a high temperature, e.g. 1550°C.

named as Pore IIa), or between alumina particle(s) and numerous small zirconia particles (inter-alumina-zirconia particle pores, named as Pore IIb), as can be seen in Fig. 1 and shown schematically in Fig. 12(A). Pores I can be removed during sintering at relatively low temperatures, while Pores IIa will not shrink appreciably due to unfavourable kinetic conditions at low temperatures with large alumina particles surrounding the pores. Thermodynamically, Pores IIb may be stable at low sintering temperatures as such pores are coordinated by many very small zirconia particles relative to the alumina particle (Fig. 12(B)), and such pores, as analyzed by Lange,<sup>29</sup> will not shrink at relatively low temperatures before the zirconia particles begin to grow substantially. With the increase of temperature, when the densification process of pure Y-TZP has been completed, Pores IIa will begin to shrink and with the growth of the zirconia particles the coordination number of Pores IIb will decrease and such pores will also become unstable and start to shrink (Fig. 12(C)). So the retarded (and enhanced) densification of the composite powder compacts at relatively low (and high) temperatures, compared to single phase Y-TZP, can be understood. As temperature increases to a certain threshold, e.g. 1550°C, both Pore IIa and Pore IIb in the compacts are removed (Fig. 11, as modelled in Fig. 12(D)) and the sintered densities were rather high when the  $\text{Al}_2\text{O}_3$  content was not higher than 30 vol.%.

However, the composite powder compact of ZA10 shows a very similar densification behavior with single phase Y-TZP. This is believed to be due to its relatively low amount of alumina. At this low content, Pores II are relatively few, and Pores IIb prevail in the compact as compared to Pores IIa. However, nano-sized zirconia grains grow readily<sup>28</sup> when heated above the calcination

temperature of 750°C. Hence the thermodynamic requirements for the shrinkage of pores IIb can be easily satisfied at a relatively low temperature of about 1050°C (Fig. 6). As a result the densification rate of ZA10 was not affected significantly.

#### 4.2 Effect of tensile back stress

The retarded densification of ceramic powder compacts with heterogeneities (inclusions), as a special example of composite powder compacts, has been modelled by calculating the hydrostatic tensile stress in the powder matrix.<sup>15-17</sup> The tensile stress is expected to oppose the sintering stress and therefore impede densification. The concept of back stress has been used<sup>10,11</sup> to explain the limited achievable final density of a composite compact of  $\text{Al}_2\text{O}_3$ , or Y-TZP with very large  $\text{Al}_2\text{O}_3$  particles of 200  $\mu\text{m}$  by local difference in density, grain size or chemical composition. The back stress concept was developed<sup>20,21</sup> for the system of large  $\text{ZrO}_2$  particles in an  $\text{Al}_2\text{O}_3$  matrix. The size ratio of secondary particles to matrix grains was higher than 100 and the large particles were irregularly shaped or even elongated. The stress caused by the inclusions in matrix may either be compressive or tensile. Densification and grain growth in the compressive region were promoted and formed a so-called non-deformable network. This non-deformable network constrained the shrinkage of the adjacent porous region by exerting tensile stress opposing densification. However, there are three ways where the effect of compressive and/or tensile back stress on densification may be limited in our system. First, the alumina particle size and the size ratio of alumina particles to Y-TZP matrix in the present system are much smaller as compared to those used by Tuan<sup>10,11</sup> and Lange,<sup>20,21</sup> although the stress arising from the secondary particles (or inclusions) is independent of their size,<sup>30</sup> nonetheless as analysed<sup>30</sup> and experimentally

observed by others, the defects (or cracks) are much easier to form around larger inclusions than around smaller. Secondly, the matrix of Y-TZP in this study is very porous and nano-sized, so the tensile stress that resulted from the  $\text{Al}_2\text{O}_3$ , during densification could be effectively absorbed and relaxed by microstructural modification (particle rearrangement, and plastic flow), especially at the initial and intermediate stage of sintering. Thirdly, the secondary  $\text{Al}_2\text{O}_3$  particles are basically equiaxed and well dispersed in matrix (Fig. 11), so the so-called non-deformable network<sup>20,21</sup> would not form in microstructure and the densification rate in the matrix is expected to be basically the same throughout the specimen.

## 5 Summary

This study shows that the densification of the Y-TZP powder compacts with the addition of alumina particles (size ratio of  $\text{Al}_2\text{O}_3$  to Y-TZP is about 10) is retarded by the presence of larger alumina particles. The alumina particles impede the shrinkage of the composites at relatively low temperature ( $\leq 1300^\circ\text{C}$ ) at which the single phase Y-TZP undergoes the major shrinkage, and lead to enhanced densification rate at and above  $1300^\circ\text{C}$ . Almost full densification is achieved at  $1550^\circ\text{C}$ . The retarded densification behavior of the composites are related to the duplex pore size distributions in the green compacts because of the presence of relatively large alumina particles. The presence of inhomogeneities, i.e. larger pores in the compacts for the composite powders, in addition to the smaller pores which the single phase Y-TZP contains, appears to be the main reason for the retarded densification of the composites from both the thermodynamic and kinetic point of view. Back stress effects resulting from secondary  $\text{Al}_2\text{O}_3$  are argued to be less significant.

## References

1. Claussen, N., Fracture toughness of  $\text{Al}_2\text{O}_3$  with unstabilized  $\text{ZrO}_2$  dispersed phase. *J. Am. Ceram. Soc.*, **59** (1976) 49.
2. Lange, F. F., Transformation toughening Part 4: Fabrication, fracture toughness and strength of  $\text{Al}_2\text{O}_3$ - $\text{ZrO}_2$  composites. *J. Mater. Sci.*, **17** (1982) 247.
3. Ruhle, M., Claussen, N. & Heuer, A. H., Transformation and microcrack toughening as complementary process in  $\text{ZrO}_2$ -toughened  $\text{Al}_2\text{O}_3$ . *J. Am. Ceram. Soc.*, **69** (1986) 195.
4. Hori, S., Yoshimura, M. & Somiya, S., Strength-toughness relations in sintered and isostatically hot pressed  $\text{ZrO}_2$ -toughened  $\text{Al}_2\text{O}_3$ . *J. Am. Ceram. Soc.*, **69** (1986) 169.
5. Tsukuma, K., Ueda, K. & Shimada, M., Strength and fracture toughness of HIPed composites of  $\text{Al}_2\text{O}_3$  and  $\text{Y}_2\text{O}_3$ -partial-stabilized  $\text{ZrO}_2$ . *J. Am. Ceram. Soc.*, **68** (1985) C-4.
6. Messing, G. L. & Onada, G. Y., Sintering of inhomogeneous binary powder mixtures. *J. Am. Ceram. Soc.*, **64** (1981) 468.
7. De Jonghe, L. C., Rahaman, M. N. & Hsueh, C. H., Transient stresses in bimodal compacts during sintering. *Acta Metall.*, **34** (1986) 1467.
8. Weiser, M. W. & De Jonghe, L. C., Inclusion size and sintering of composite powders. *J. Am. Ceram. Soc.*, **71** (1988) C-125.
9. Rahaman, M. N. & De Jonghe, L. C., Sintering of particulate composites under a uniaxial stress. *J. Am. Ceram. Soc.*, **73** (1990) 602.
10. Tuan, W. H., Gilbert, E. & Brook, R. J., Sintering of heterogeneous ceramic composites, Part I,  $\text{Al}_2\text{O}_3$ - $\text{Al}_2\text{O}_3$ . *J. Mater. Sci.*, **24** (1989) 1062.
11. Tuan, W. H. & Brook, R. J., Sintering of heterogeneous composites, Part II,  $\text{ZrO}_2$ - $\text{Al}_2\text{O}_3$ . *J. Mater. Sci.*, **24** (1989) 1953.
12. Bordia, R. K. & Raj, R., Sintering of  $\text{TiO}_2$ - $\text{Al}_2\text{O}_3$  composites: a model experimental investigation. *J. Am. Ceram. Soc.*, **71** (1988) 302.
13. Sudre, O. & Lange, F. F., Effect of inclusions on densification: I, Microstructural development in an  $\text{Al}_2\text{O}_3$  matrix containing a high volume fraction of  $\text{ZrO}_2$  inclusions. *J. Am. Ceram. Soc.*, **75** (1992) 519.
14. Scherer, G. W., Viscous sintering of a bimodal pore size distributions. *J. Am. Ceram. Soc.*, **67** (1984) 709.
15. Hsueh, C. H., Sintering behaviour of powder compacts with multi-heterogeneities. *J. Mater. Sci.*, **21** (1986) 2067.
16. Hsueh, C. H., Influence of multiple heterogeneities on sintering rates. *J. Am. Ceram. Soc.*, **69** (1986) C-64.
17. Scherer, G. W., Sintering with rigid inclusions. *J. Am. Ceram. Soc.*, **70** (1987) 719.
18. Bordia, R. K. & Scherer, G. W., On constrained sintering. I, II, III, Overview No. 70, *Acta Met.*, **36** (1988), 2392, 2399, 2411.
19. Lange, F. F., Densification of powder rings constrained by dense cylindrical cores. *Acta Metall.*, **37** (1989) 697.
20. Lange, F. F., Constrained network model for predicting densification behavior of composite powders. *J. Mater. Res.*, **2** (1987) 59.
21. Sudre, O., Bao, G., Fan, B., Lange, F. F. & Evans, A. G., Effect of inclusions on densification: II, Numerical model. *J. Am. Ceram. Soc.*, **75** (1992) 525.
22. Lange, F. F. & Hirlinger, M. M., Grain growth in two phase ceramics, alumina inclusions in Zirconia. *J. Am. Ceram. Soc.*, **70** (1987) 827.
23. Lange, F. F., Yamaguchi, T., Davis, B. I. & Morgan, P. E. D., Effect of  $\text{ZrO}_2$  inclusions on the sinterability of  $\text{Al}_2\text{O}_3$ . *J. Am. Ceram. Soc.*, **71** (1988) 446.
24. Lange, F. F. & Kellett, B. J., Thermodynamics of densification: II, Grain growth in porous compacts and relation to densification. *J. Am. Ceram. Soc.*, **72** (1989) 735.
25. Chen-Lung Fan & Rahaman, M. N., Factors controlling the sintering of ceramic particulate composites I, Conventional processing. *J. Am. Ceram. Soc.*, **95** (1992) 2056.
26. Ching-Li Hu & Rahaman, M. N., Factors controlling the sintering of ceramic particulate composites II, coated inclusion particles. *J. Am. Ceram. Soc.*, **75** (1992) 2066.
27. Shi, J. L., Characteristics of the pore structures in the compacts of ultrafine zirconia powders. *J. Solid State Chem.*, **95** (1992) 412.
28. Shi, J. L., Lin, Z. X. & Yen, T. S., Determination of crystallite size of superfine zirconia powders as a function of calcination temperature. *Ceram. Int.*, **18** (1992) 155.
29. Lange, F. F., Sinterability of agglomerated powder. *J. Am. Ceram. Soc.*, **65** (1982) 83.
30. Lange, F. F., Criteria for crack extension and arrest in residual, localised stress fields associated with second phase particles. In *Fracture Mechanics Vol. 2, Microstructures, Materials and Applications*, ed. R. C. Bradt & D. P. H. Hasselman. Plenum, New York, 1974, p. 599.